ADVANCED THERAPEUTICS
www.advtherap.com

Translational mRNA Profiling Analysis of Pseudopalisading Cells in Bevacizumab Resistance of GBM

Yejin Kim, Tae Hoon Kim, Srun Sreynet, Yong Seok Oh, Do-Hyun Nam, Jong Bae Park,* and Sung Soo Kim**

Glioblastoma (GBM) is a malignant brain tumor with a poor prognosis that easily recurs. The antiangiogenic agent bevacizumab is used to treat recurrent GBM. However, GBM treated with bevacizumab easily rebounds due to evasive mechanisms that induce resistance to treatment, such as hypoxia-inducible factor (HIF) associated pathways. The transcription factor HIFs are oxygen-dependent and are degraded via the ubiquitin-dependent proteasomal pathway. Therefore, it is necessary to study bevacizumab resistance with HIF-associated pathways through translational mRNA profiling. This work applies a hypoxia response element (HRE) promoter to the ribosome affinity purification (TRAP) system for hypoxia-specific translational mRNA profiling analysis. Here, this work analyzes the translatome of pseudopalisading cells in the brain samples of orthotopic mouse models using hypoxia-responsive 5× HRE-TRAP system to investigate the molecular mechanism of drug resistance on pseudopalisading cells around the necrotic area induced by bevacizumab resistance. The translatomic analysis result shows that pseudopalisading cells exhibit notable enrichment of gene sets associated with neurodegenerative diseases, such as Alzheimer's disease. The outcomes of this study enhance clinical relevance, meaning that the translatomic analysis result of pseudopalisading cells during bevacizumab treatment-induced resistance provides new insight into a promising approach for developing targeted therapeutics.

1. Introduction

Glioblastoma (GBM) is an aggressive type of brain tumor that is difficult to treat, and there is a high rate of recurrence after initial treatment.[1,2] Bevacizumab, a monoclonal antibody that inhibits the activity of VEGF,[3] has been used in the treatment of recurrent GBM with the goal of reducing the growth of blood vessels that supply the tumor. However, it showed the effect on the progression of the disease but not on the overall survival of patients.[4–6] The VEGF-related pathway is blocked to induce tumor hypoxia. This, in turn, triggers activation of the hypoxia-inducible factor (HIF) associated pathways within a low oxygen environment, thereby promoting resistance.[7,8]

Pseudopalisading cells are a hallmark feature of GBM, a highly aggressive type of brain tumor.[9,10] Pseudopalisading cells are found around areas of tumor necrosis, where cells have died due to insufficient blood supply. The pseudopalisading cells are characterized by elongated nuclei arranged in a radial pattern, and they are thought to be involved in acquiring drug resistance and recurrence by the migration and invasion of tumor cells with secreting malignancy factors.[11]

Translational ribosome affinity purification (TRAP) is a technique used to isolate and identify the actively translating mRNAs from a specific cell type or tissue. The method relies on the fact that ribosomes are responsible for translating mRNA into proteins and that they remain bound to the mRNA during translation.[12] The TRAP system involves genetically modifying a particular cell type or tissue to express a tagged ribosomal

Y. Kim, T. H. Kim, S. Sreynet, J. B. Park, S. S. Kim
Graduate School of Cancer Science and Policy
National Cancer Center
Goyang 10408, Republic of Korea
E-mail: jbp@ncc.re.kr; kss@ncc.re.kr

The ORCID identification number(s) for the author(s) of this article can be found under https://doi.org/10.1002/adtp.202300148

DOI: 10.1002/adtp.202300148

Y. Kim, D.-H. Nam
Department of Health Sciences and Technology
SAIHST
Sungkyunkwan University
Seoul 06355, Republic of Korea
E-mail: nsnam@skku.edu

Y. S. Oh
Department of Brain-Cognitive Science
Daegu-Gyeongbuk Institute of Science and Technology (DGIST)
Hyenpung-myeon, Dalseong-gun, Daegu 42988, Republic of Korea

D.-H. Nam
Department of Neurosurgery
Samsung Medical Center
Sungkyunkwan University School of Medicine
Seoul 06531, Republic of Korea

protein, which can be used to selectively isolate the ribosomes and their associated mRNAs. The tagged ribosomal protein can be expressed using a cell-specific promoter, ensuring that only the targeted cells express the tag. The isolation of ribosomes and their associated mRNAs is achieved by using antibodies or other affinity molecules that recognize and bind to the tag on the ribosomal protein L10a. This allows for the purification of the ribosomes and their associated mRNAs from a complex mixture of cellular components. Once the ribosomes and their associated mRNAs are isolated, the mRNAs can be identified and characterized using techniques such as microarray analysis or RNA sequencing.[13–15] This allows researchers to identify the genes that are actively being translated in a specific cell type or tissue and to gain insights into the functional and regulatory properties of these genes. TRAP has been used in a variety of research applications, including the study of gene expression in specific cell types, the identification of novel genes involved in disease states, and the discovery of new drug targets especially in the nervous system.[16]

In this study, we analyzed the IVY GAP data of GBM patients based on tumor location to explore potential factors contributing to the malignant progression of GBM. We found that gene sets associated with the hypoxic tumor microenvironment were enriched in pseudopalisading cells, accompanied by HIF-associated pathways. Additionally, we established a GBM orthotopic mouse model using HIF-associated pathways for translational mRNA profiling. We applied a hypoxia response element (HRE) promoter that included a 5× HRE-TRAP system and treated it with bevacizumab to analyze the translatomic changes in pseudopalisading cells under the hypoxic tumor environment induced by bevacizumab resistance. The results showed enrichment of gene sets associated with neurodegenerative diseases and cancer malignancy signatures compared to bulky RNA sequecing and proteomic analysis results in vitro. The findings show significant clinical relevance underlying pseudopalisading cell-mediated malignancy. Our 5× HRE-TRAP system provides new insights into the development of new therapeutic strategies for GBM.

2. Results and Discussion

2.1. Enhancement of Hypoxia-Associated Gene Sets in Pseudopalisading Cells by Geographic Tumor Location-Based Classification

To investigate the potent malignancy factors that distinguish geographic tumor location in GBM, we analyzed data from 104 GBM patients in the IVY GAP data bank. The transcriptomic data of the patients were classified based on five geographic tumor location characteristics, including cellular tumor, infiltration tumor, leading edge, microvascular proliferation, and pseudopalisading cells.[17] Through the analysis, we found that pseudopalisading cells were uniquely distinguished by enriched gene sets related to the hypoxic tumor microenvironment (**Figure 1**A). Furthermore, pseudopalisading cells exhibited upregulated HIF-associated pathways, including signatures of apoptosis, glycolysis, adipogenesis, and mTOR signaling (Figure S1, Supporting Information). Taken together, we concluded that the pseudopalisading cells associated with HIFs pathways under the hypoxic environment are an important malignant factor in GBM.

Bevacizumab enhances hypoxic conditions by regulating angiogenesis and the role of hypoxia as a crucial factor in driving tumor adaptation, promoting tumor progression, and therapeutic resistance, has been widely established.[7,8] Specifically, the presence of hypoxia and its related factors, such as HIF-1α, have been linked to the formation of pseudopalisading necrotic regions, which serve to safeguard the stem cell niche and thereby contribute to the aggressive phenotype of these tumors.[18] Therefore, we investigated the effect of the hypoxic conditions induced by bevacizumab treatment on pseudopalisading cells in GBM. The result suggests that the pseudopalisading cells are considered an essential factor in the tumor microenvironment to trigger GBM progression.

2.2. Establishment of the 5× HRE-TRAP System Under Hypoxic Conditions In Vitro

To investigate the translatome affected by hypoxia in pseudopalisading cells, we established a hypoxic condition responsive 5× HRE-TRAP system that specifically activates under hypoxic conditions. As the transcription regulator HIFs activating the transcripts are easily degraded via the ubiquitin-dependent proteasomal pathway, we inserted 5× HRE sequences next to the cytomegalovirus (CMV) promoter of the TRAP vector. In addition, for tagging, we placed the GFP sequence next to the human ribosomal subunit hrpL10a. When intracellular oxygen becomes deficient and a hypoxic environment is generated, the translatome produced in that environment are tagged by rRNA-GFP fusion. Afterward, GFP-hrpL10a was precipitated using GFP-specific antibodies, enabling translatomic analysis by isolating the ribosomes and their associated translational mRNAs under hypoxic conditions (**Figure 2**A).

We applied the 5× HRE-TRAP system activating under hypoxic conditions to assess the regulatory roles of pseudopalisading cells in the malignant transition of GBM in vitro. The system was transfected into U87MG and glioma stem cell (GSC) 83NS cells, and its systemic operation was validated. The immunostaining result shows that the 5× HRE-TRAP system was specifically activated in the hypoxic condition (1% oxygen) not in the normoxia condition (22% oxygen), as shown by the expression of HIF-1α and endogenous GFP in stable U87MG and GSC 83NS cell lines (Figure 2B and Figure S2, Supporting Information). Additionally, the hypoxic condition responsive GFP expressions were specifically analyzed by flow cytometry in GBM cells, and strong expressions were detected in the hypoxic condition (1% oxygen) in the cells (Figure 2C). Furthermore, the HRE-TRAP system was validated by the detection of shifted-up bands of GFP-hrpL10a compared to GFP in western blotting under hypoxic conditions (Figure 2D).

Taken together, we confirmed that the 5× HRE-TRAP system specifically operates under hypoxic conditions and identifies the comprehensive ribosomal proteins that are translated under low-oxygen levels. This demonstration establishes that a 5× HRE-TRAP system is a reliable tool for elucidating the regulatory roles of pseudopalisading cells in GBM.

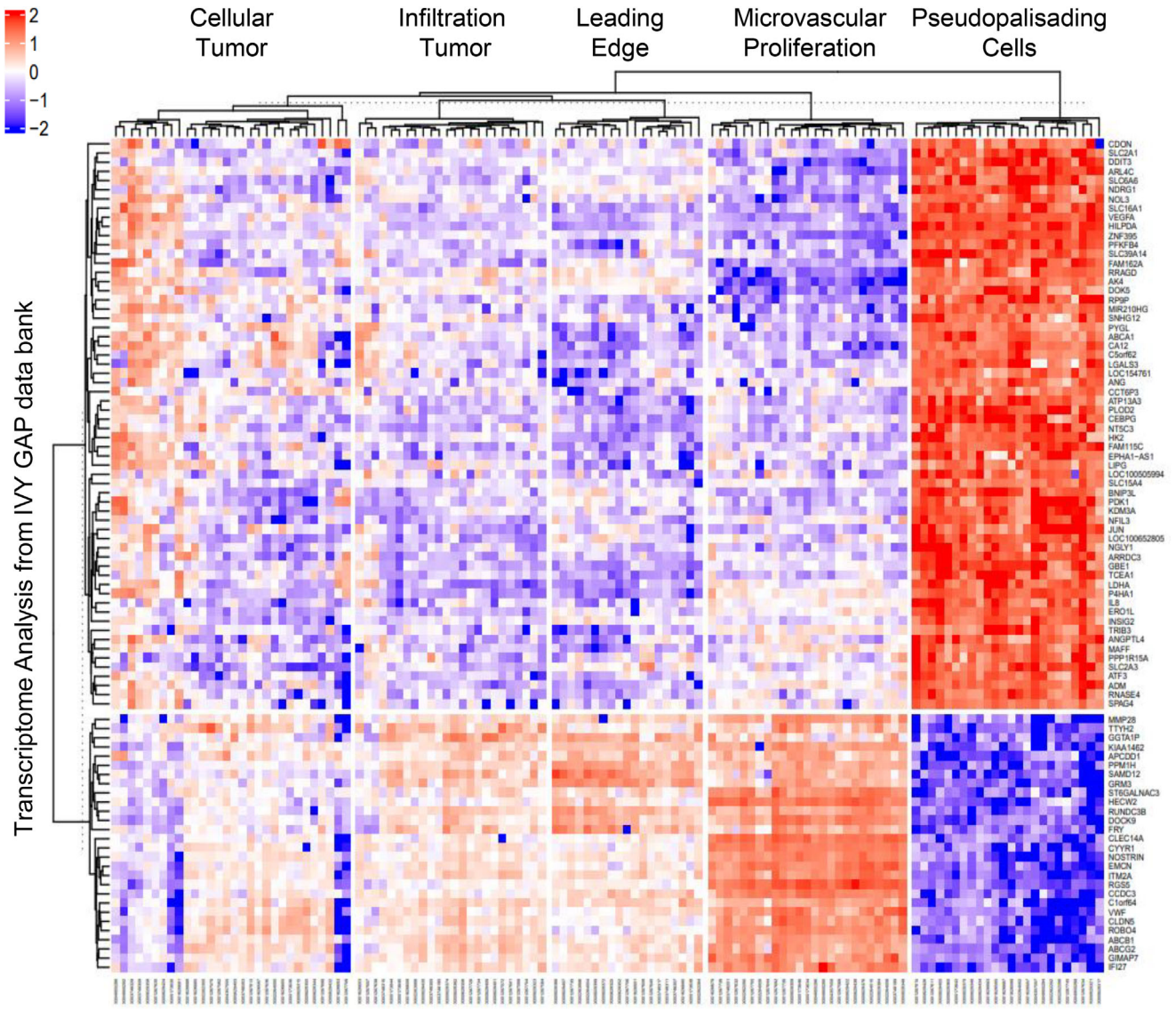

Figure 1. Geographic tumor location-based classification of IVY GAP glioblastoma (GBM) patients' data. A heatmap of transcriptomic analysis of IVY GAP GBM data. The data of 104 GBM patients were analyzed by the tumor location; cellular tumor, infiltration tumor, leading edge, microvascular proliferation, and pseudopalisading cells.

2.3. Establishment of the 5× HRE-TRAP System Under Hypoxic Conditions In Vivo

To assess the regulatory roles of pseudopalisading cells and associated translatomic changes during the resistance transition of GBM induced by bevacizumab treatment, we established an orthotopic xenograft model of GBM. The GBM cells were transfected with the hypoxic condition responsive 5× HRE-TRAP system. As we expected, the expression of endogenous GFP was predominantly observed in pseudopalisading cells surrounding necrotic regions in the bevacizumab-treated tumors, compared to the vehicle-treated tumors of the U87MG and GSC 83NS xenograft models (**Figure 3**A and Figure S3A,F, Supporting Information). Following this, brain tissues were homogenized, and the translatome was isolated by immunoprecipitation using a specific anti-GFP antibody in the elution samples. Immunoblot (IB) analysis revealed enriched shifted-up bands of eGFP-hrpL10a in the bevacizumab-treated brains compared to the vehicle-treated brains, indicating that bevacizumab treatment induces a hypoxic environment that activates the 5× HRE-TRAP system in brain tumors. Specifically, the enriched shifted-up bands of eGFP-hrpL10a are detected in the elution samples, not in the supernatant of the brain samples (Figure 3B). Moreover, the expression of endogenous GFP was confirmed in bevacizumab-treated brain tumors of 5 ×HRE-TRAP transfected U87MG brain samples, while GFP expression was detected in both vehicle- and bevacizumab-treated CMV-promoter vector-transfected brain samples. Additionally, elevated enriched expressions of HIF-1α were observed in 5× HRE-TRAP transfected brain samples compared to the bevacizumab-treated naïve and

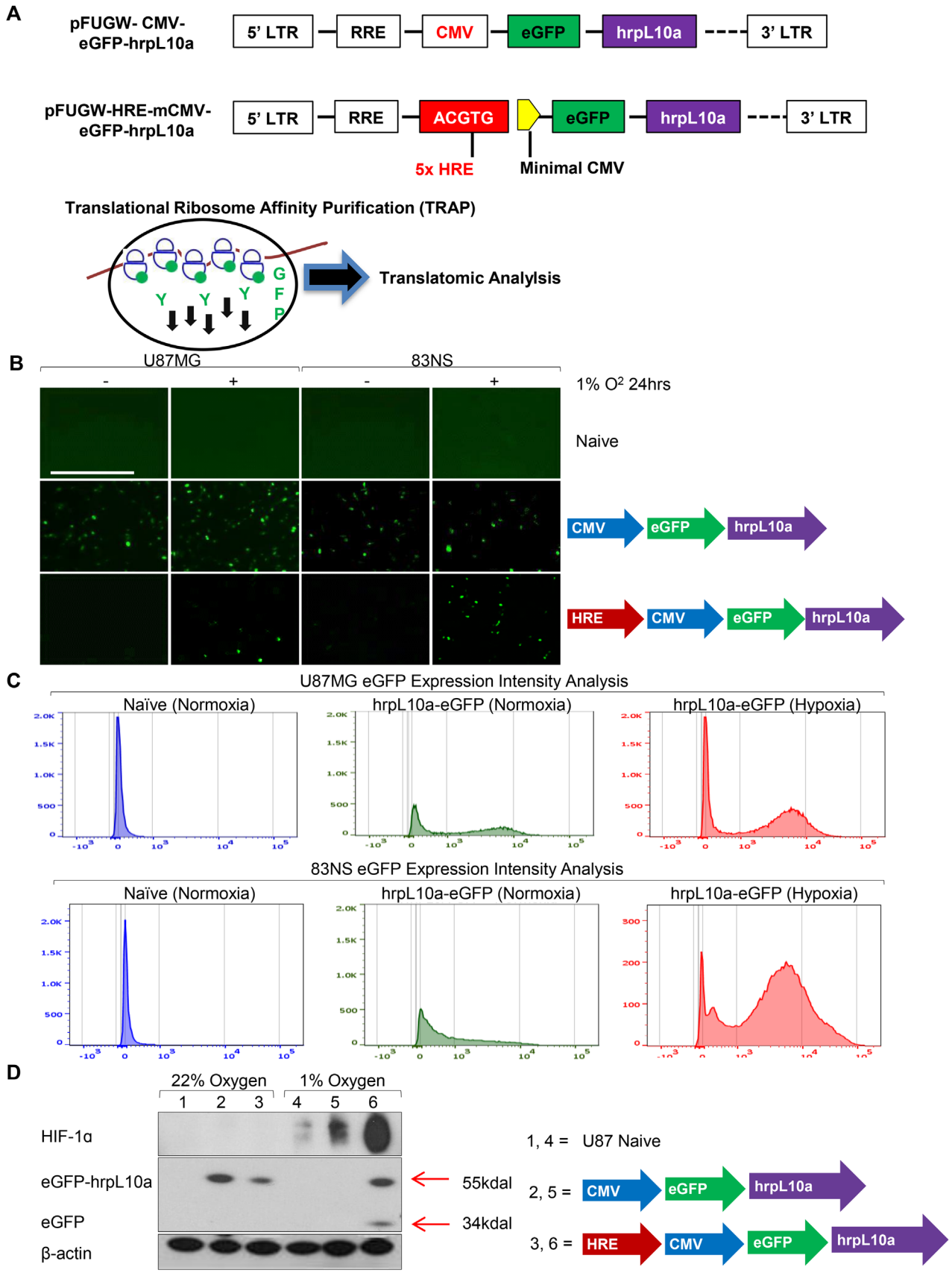

Figure 2. Establishment and validation of the 5× HRE-TRAP system in vitro. A) Schematic graphical abstract of 5× HRE-TRAP system. 5× hypoxia response element (HRE) sequences were conjugated next to the cytomegalovirus (CMV) promoter. The GFP sequence was placed as a tag. The system marks GFP on the ribosomal protein under hypoxic conditions. B) Representative immunocytochemistry (ICC) images of endogenous GFP expression were obtained from U87MG and glioma stem cell (GSC) 83NS cells transfected with the 5× HRE-TRAP system and cultured under 1% oxygen for 24 h. Magnification 20×; Scale bar, 100 μm. C) A representative histogram of flow cytometry analysis showing the intensity of endogenous GFP expression in U87MG and GSC 83NS cells transfected with the 5× HRE-TRAP system under 1% and 22% oxygen. D) Immunoblot (IB) analysis of HIF-1α and GFP-hrpL10a expression in naïve U87MG, TRAP, or 5× HRE-TRAP vector transfected U87MG cells cultured under 1% and 22% oxygen. β-actin was used as a control.

CMV vector-transfected brain samples (Figure S3B,C, Supporting Information), confirming the induction of a hypoxic environment by bevacizumab treatment. Furthermore, we explored the translational mRNAs obtained from 5× HRE-TRAP transfected U87MG orthotopic xenograft brain tumors treated with vehicle or bevacizumab. RT-PCR analysis of the purified translatome samples revealed enriched expression hypoxia-related markers, such as CA9, NDRG1, and VEGF (Figure S3D, Supporting Information). Additionally, the brain tissues treated with bevacizumab in GSC 83NS cells showed elevated expression of the hypoxia condition marker HIF-1α and hypoxia-related malignant progression markers, including CEBP/β and pSTAT3 (Figure S3E, Supporting Information). These findings provide further evidence that bevacizumab treatment induces hypoxia and influences the progression of malignancy in the GBM orthotopic model.[19]

In conclusion, our findings suggest that a 5× HRE-TRAP system is a valuable tool for analyzing translatomic changes occurring in pseudopalisading cells surrounding the necrotic areas

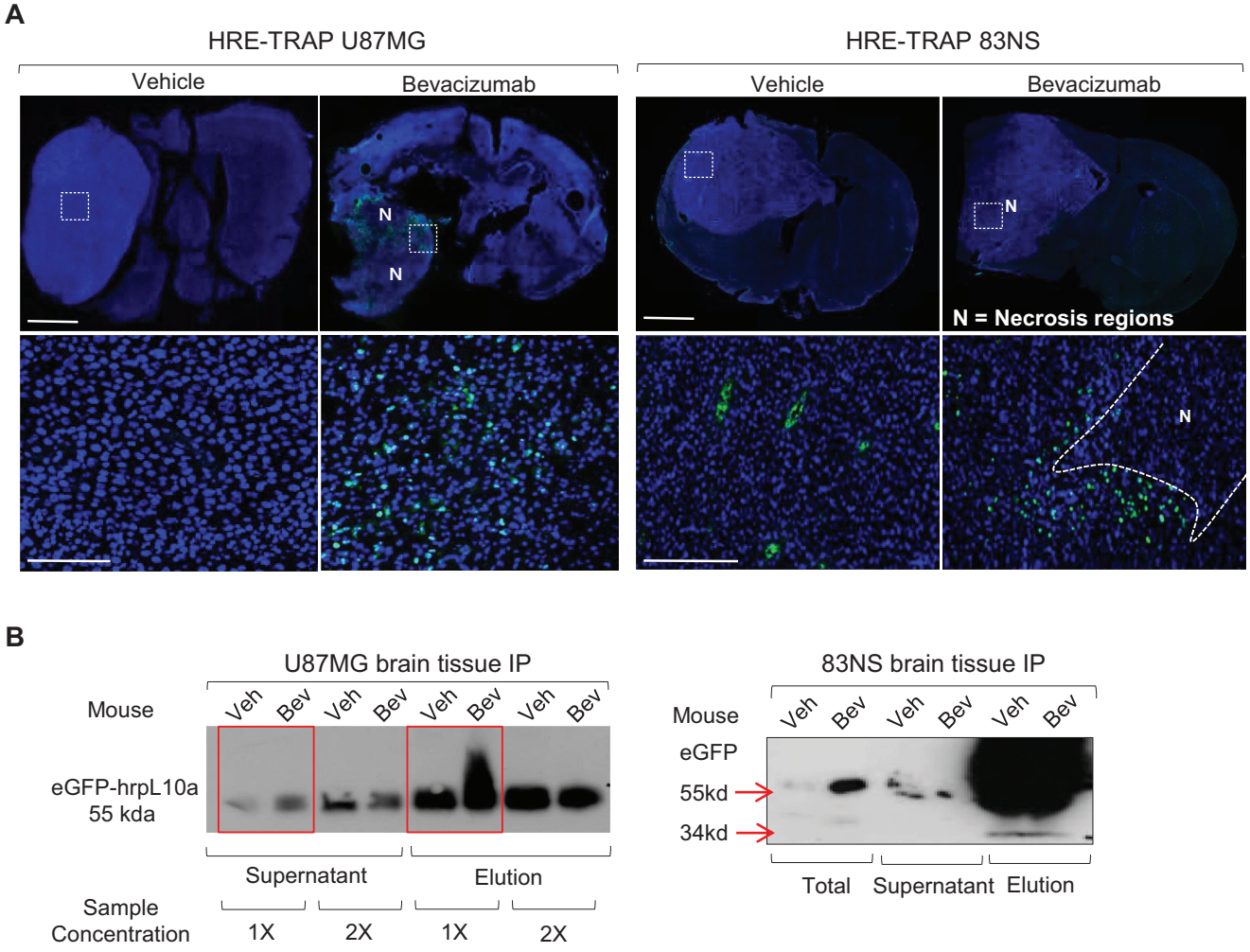

Figure 3. Establishment and validation of hypoxic condition responsive 5× HRE-TRAP system in vivo. A) Representative immunofluorescence images of endogenous GFP in the brain tissues of 5× HRE-TRAP system transfected U87MG and glioma stem cell (GSC) 83NS xenograft mice treated with vehicle or bevacizumab (10 mg kg^{-1}). The brains were harvested at 5.5 weeks and homogenized for analyzing translatome, N = necrosis, and the brain tumors were marked with a white dotted line. Scale bar, 100 μm (above), 100 μm (below). B) Immunoblot (IB) analysis of eGFP-hrpL10a fusion proteins in the brain tissues of 5× HRE-TRAP transfected U87MG and GSC 83NS xenograft brain. The brains were homogenized and pulled down with a specific anti-GFP antibody.

under the hypoxic microenvironment induced by bevacizumab treatment in GBM. This system allows for labeling ribosomal proteins and mRNA, facilitating the study of regulatory processes involved in bevacizumab resistance.

2.4. Translatomic Analysis in the Brain Tissues of GSC 83NS Transfected with Hypoxic Condition Responsive 5× HRE-TRAP System

To analyze the clinical relevance of bevacizumab treatment on translatomic changes in human GSC 83NS cells transfected with the 5× HRE-TRAP system, we conducted a comprehensive translatomic analysis of brain tissues treated with vehicle or bevacizumab. The brain tissues extracted from the bevacizumab-treated mice were homogenized and precipitated by streptavidin beads with GFP-specific antibodies to analyze the translatome. The result of the translatomic analysis revealed that gene sets associated with neurodegenerative diseases and cancer-related signatures were enriched with 1.5-fold changes (Figure S4A, Supporting Information). We validated our enriched gene sets of the 1.5-fold data in the TCGA GBM database, and the result showed a significant correlation with the translatomic analysis and clinical meaning. Specifically, the upregulated gene sets enriched GBM patients show poor survival benefits compared to the downregulated gene sets enriched GBM patients in disease-free survival (DFS) and overall survival (**Figure 4**D). However, the result of the translatomic analysis revealed that conventinoal malignancy gene sets such as proliferation, invasion, and EMT were enriched with 2.0-fold changes. Human GSC 83NS cells transfected with the 5× HRE-TRAP system in vitro and the gene sets of the two fold data showed poor clinical relevance between the expression of gene sets and the TCGA GBM database (Figure 4A,B). Strikingly, in vitro, translatomic, and proteomic analysis results show less clinical relevance compared to the comprehensive translatomic analysis results of the 5× HRE-TRAP 83NS brain tissues treated with vehicle or bevacizumab. The result shows poor clinical relevance in the TCGA GBM database (Figure S4A,B, Supporting Information).

3. Conclusion

In this study, we investigated the role of pseudopalisading cells in GBM malignancy, specifically their relationship between the hypoxic tumor microenvironment and bevacizumab resistance. We utilized a hypoxic condition responsive 5× HRE-TRAP system to investigate the regulatory roles of pseudopalisading cells and their associated translatomic changes in malignant transition. Treatment with bevacizumab enhances hypoxic conditions and promotes pseudopalisading cell transformation in GBM. In addition, the enrichment of gene sets induced by bevacizumab resistance is related to neurodegenerative diseases and cancer malignancy signatures suggesting significant clinical relevance underlying pseudopalisading cell-mediated malignancy. The findings clarify the molecular mechanisms underlying pseudopalisading cell-mediated malignancy and may inform the development of new therapeutic strategies for GBM with bevacizumab resistance.

4. Experimental Section

Cell Culture: The cells were maintained as previously described.[20] The U87MG cells were cultured in Dulbecco's modified Eagle's medium (DMEM) containing 10% fetal bovine serum (HyClone). The patient-derived glioma stem cells, 83NS, were cultured in DMEM/F-12 supplemented with B27 (Invitrogen), EGF (10 ng mL^{-1}, R&D Systems), and bFGF (5 ng mL^{-1}, R&D Systems), along with penicillin/streptomycin at a concentration of 1×.

Lentivirus Production and Infection: Lentiviruses were produced following a previously reported method.[21,22] Briefly, 6×10^6 293T cells were plated onto 100-mm culture dishes, incubated for 24 h, and then co-transfected with 4.5 μg of TRAP lentiviral constructs,[12] 3 μg of psPAX2 (Addgene), and 1.5 μg of pMD2.G (Addgene) using 27 μL of Lipofectamine 2000 (Invitrogen). The medium was changed 6 h later, and 48 h after transfection, the medium containing lentivirus was harvested. Viral particles were then concentrated and purified using a Lenti-X concentrator (Clontech). To infect the cells, the lentivirus was added in the presence of 10 μg mL^{-1} polybrene.

TRAP: The TRAP constructs were generated by inserting hrpL10a with an N-terminal Not-I site following the ATG in pFUGW using EcoRI/XbaI.[12] Then, a cassette containing Not-I flanked GFP (TRAP) was inserted, and the resulting construct was assessed by Western blot against GFP. Brain dissections were performed in dissection buffer (1× HBSS, 2.5×10^{-3} M HEPES [pH 7.4], 35×10^{-3} M glucose, 4×10^{-3} M NaHCO3) containing 100 μg mL^{-1} of cycloheximide (CHX). The central brain was discarded, and the optic lobes and retina were frozen on dry ice and stored at −80 °C in lysis buffer (20×10^{-3} M HEPES [pH 7.4], 150×10^{-3} M KCl, 5×10^{-3} M MgCl with protease inhibitors) containing 100 μg mL^{-1} CHX until enough optic lobes were accumulated.

For each replicate using the Chp-GAL4 driver, 40 optic lobes were used.

Endogenous GFP Imaging: U87MG and GSC 83NS were grown on 96-well (CellCarrer-96 Ultra Microplates, black, 96-well with lid case. After 72 h, cells were fixed at 4% paraformaldehyde (PFA). Fluorescence images were obtained using an Operetta CLS (PerkinElmer).

LC–MS/MS Analysis and Data Processing: LC–MS/MS analysis and data processing were performed as previously described.[23] Briefly, samples were separated using in-house packed analytical and trap columns, with a linear gradient ranging from 95% solvent A to 40% solvent B and a flow rate of 300 nL min^{-1} over a 2-h period. The enriched samples were sequenced using an Orbitrap Fusion Lumos mass spectrometer. For the transiently expressed ContactID in HEK293T, cells were induced and transfected with plasmids using Lipofectamine 2000, then biotinylated with 50×10^{-6} M of biotin. The lysates were clarified by ultrasonication, and the two T75 flask samples were combined. The pellet was resolubilized with 1 mL of 8 M urea in 50×10^{-3} M ammonium bicarbonate, and the protein concentration was determined using a BCA assay. Samples were digested with trypsin after denaturation, reduction, and alkylation. Biotinylated peptides were heated and mixed with acetonitrile, TFA, and formic acid, and elution was repeated five times. The elution fractions were combined, dried using Speed vac, and stored at −20 °C or directly injected to mass spectrometry.

The study utilized MaxQuant software and the Andromeda search engine to search MS/MS data against the SwissProt Homo sapiens proteome database with specific search parameters, achieving an FDR of less than 1%. LFQ intensity values were log-transformed, and missing values were imputed using a normal distribution, with a Gaussian distribution created for the total matrix. The raw proteomics analysis data is available on ProteomeXchange consortivum via MassIVE repository and can be downloaded using the provided link and accession number (https://massive.ucsd.edu/ProteoSAFe/static/massive.jsp) (accession no. PDX015534/MSV000084362). (Download Link: ftp://massive.ucsd.edu/MSV000084362/).

Reverse Transcription-Polymerase Chain Reaction: Both semiquantitative and real-time RT-PCR were performed to determine mRNA levels as previously described.[23] Total RNA was extracted from cells using TRIzol reagent (Invitrogen) following the manufacturer's instructions, and 500 ng of the extracted RNA was used to synthesize cDNA with M-MLV reverse

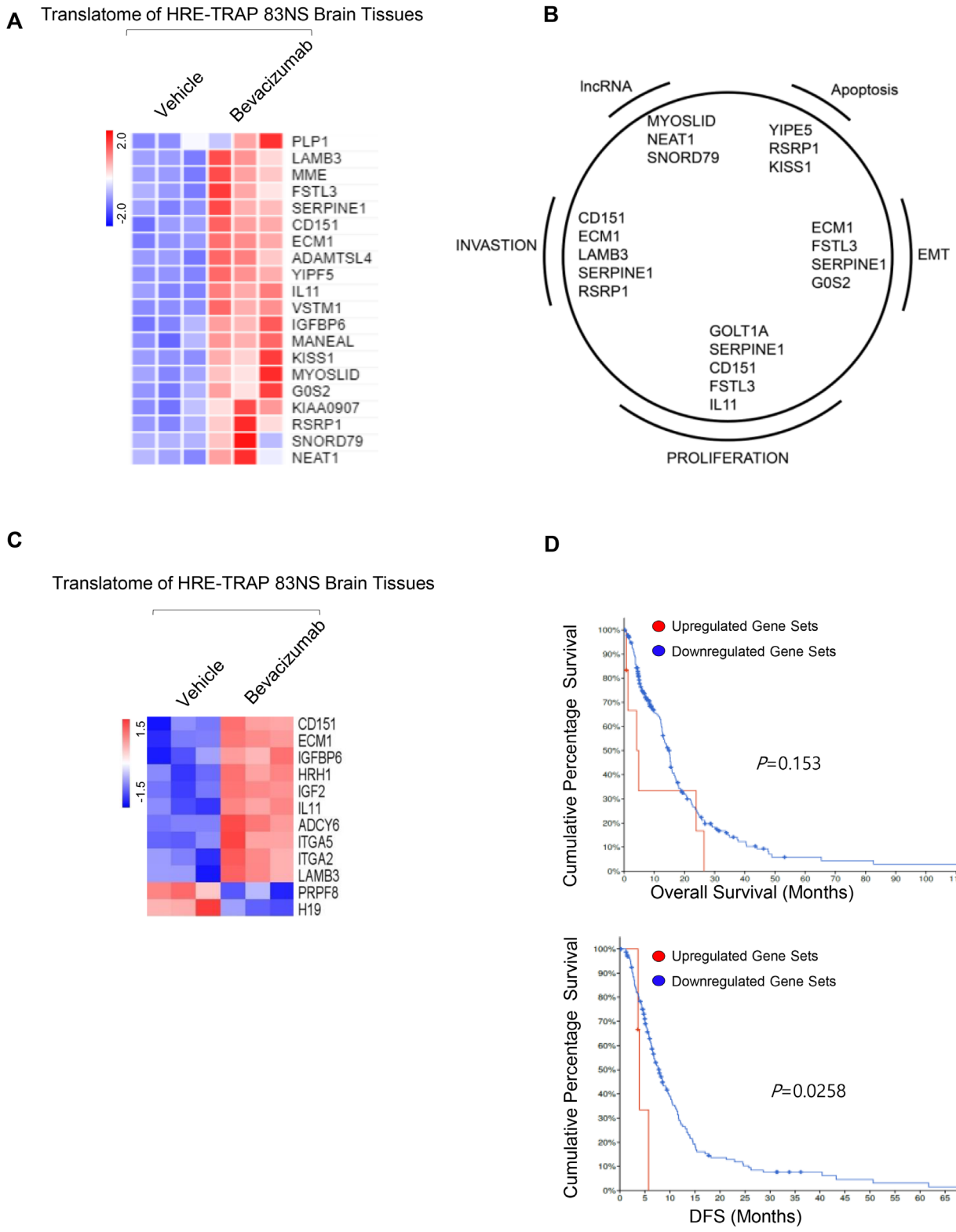

Figure 4. Translatomic analysis in the brain tissues of glioma stem cell (GSC) 83NS transfected with hypoxic condition responsive 5× HRE-TRAP system. A) A heat map of translatomic analysis from brain tissues of GSC 83NS transfected HRE-TRAP treated with vehicle or bevacizumab (fold changes ±2.0). B) A diagram of translatomic analysis from brain tissues of GSC 83NS transfected HRE-TRAP treated with vehicle or bevacizumab (fold changes ±2.0). C) A heat map of translatomic analysis results from brain tissues of GSC 83NS transfected HRE-TRAP treated with vehicle or bevacizumab (fold changes ±1.5). D) Kaplan–Meier survival analysis of the high-ranked gene lists in TCGA glioblastoma (GBM) data bank from the translatomic analysis result (fold changes ±1.5).

transcriptase (Promega). Real-time RT-PCR was conducted on a LightCycler 480II real-time detection system (Roche) using LightCycler 480 SYBR Green I Master Mix (Roche). The expression levels of the target genes were normalized to the input signal. Semi-quantitative RT-PCR products were visualized on a 1% agarose gel. The PCR primers are shown as follows: CA9, sense 5′- GACCTTGTTGGAATGGCTCTT-3′ and antisense 5′-TGGATTCAGGTGCAAATGCAA-3′; GLUT1, sense 5′-GCCAGAAGGAGTCAGGTTCAA-3′ and antisense 5′- TCCTCGGAAAGGAGTTAGATCC-3′; VEGF, sense 5′-GAGGAGCAGTTACGGTCTGTG-3′ and antisense 5′- TCCTTTCCTTAGCTGACACTTGT-3′; VEGFA, sense 5′-AGGGCAGAATCATCACGAAGT-3′ and antisense 5′-AGGGTCTCGATTGGATGGCA-3′; GFP, sense 5′- AACTACCATGTTCCTCGAACGA-3′ and antisense 5′-CTCCATCAAATCCCACACCAG-3′.

Immunoblot Analysis: The analysis was performed as previously described.[24] Proteins were extracted using RIPA buffer containing complete protease inhibitors (Roche), separated by electrophoresis, and transferred to PVDF membranes (Millipore). The membranes were then blocked with 5% skim milk (BD). Primary antibodies against HIF-1a (BETHYL, 1:1000), GFP (Abcam, 1:1000), and β-actin (Santa Cruz Biotech, sc-517582, 1:1000) were incubated overnight at 4 °C. The immunoreactive bands were visualized using peroxidase-labeled affinity-purified secondary antibodies (KPL) and the Amersham ECL prime Western blotting detection reagent (GE Healthcare).

Flow Cytometry: For intracellular marker analysis, live cells were resuspended in 0.1% BSA 1× PBS. Cells were fixed and permeabilized (Cytofix/cytoperm, BD) for intracellular GFP protein. Data were acquired by the BD LSRFortessa and analyzed with FACS Diva and FlowJo software.

Immunohistochemistry: The study was performed as previously described.[25] To observe histological features, brains were extracted, fixed in 4% PFA for 24 h at 4 °C, sectioned at a thickness of 4 µm using a Leica RM2125 RTS microtome, and stained with hematoxylin (Dako) and 0.25% eosin (Merck). Prior to immunohistochemical and immunofluorescence staining for HIF-1α (BETHYL, 1:300), the sections were subjected to an antigen retrieval process using citrate buffer (pH 6.0), and endogenous peroxidase was blocked by incubating with 3% hydrogen peroxide. Tissue sections were then incubated overnight at 4 °C in a humidified chamber with primary antibodies diluted with antibody diluent buffer (IHC World). For immunofluorescence staining, sections were obtained using an LSM 780 confocal laser-scanning microscope (Carl Zeiss).

RNA-Sequencing Data Processing: The analysis was performed as previously described.[23] RNA-Seq libraries were prepared using the TruSeq RNA Library Prep kit (Illumina) and were submitted for transcriptome resequencing. To ensure high-quality raw FASTQ files, the Phred quality score was checked using FastQC (www.bioinformatics.babraham.ac.uk/projects/fastqc). The sequences to the hg19 and GRCh37 human genome were mapped using Subread aligners (v1.5.3)48 and each resulting SAM file was analyzed using featureCounts49 and SeqMonk software (v1.38.2, www.bioinformatics.babraham.ac.uk/projects/seqmonk). Differentially expressed genes (DEGs) were identified by normalizing and quantifying read counts generated from featureCounts using the LPEseq package50, which was designed for nonreplicated samples, and the RNA-Seq quantification pipeline of Seq-Monk. Significant DEGs were chosen based on statistical significance (*p*-value and *q*-value) and fold-change. The resulting DEG graphs were visualized using the Multiple Experiment Viewer (MeV; v4.9.0)51 of the TM4 software suite. For the construction of cDNA libraries with the TruSeq Stranded mRNA kit, this work used 1 µg of total RNA and followed a protocol consisting of polyA-selected RNA extraction, RNA fragmentation, random hexamer primed reverse transcription, and 100 nt paired-end sequencing by Illumina HiSeq4000. The libraries were quantified using qPCR and qualified using an Agilent Technologies 2100 Bioanalyzer. To preprocess the raw reads from the sequencer and remove low-quality and adapter sequences before analysis, the processed reads were aligned using HISAT v2.0.552, which generated spliced alignments several times faster than Bowtie and BWA. The reference genome sequence and annotation data were downloaded from the UCSC table browser (http://genome.uscs.edu). After alignment, this work used StringTie v1.3.3b to assemble aligned reads into transcripts and estimate their abundance, providing the relative abundance estimates as FPKM values (Fragments Per Kilobase of exon per Million fragments mapped) of transcript and gene expressed in each sample. FPKM values had already been normalized with respect to library size, so this work used these values for the comparative analysis of DEGs between samples.

GBM patients' data was analyzed according to tumor location-based classification from IVY Glioblastoma Atlas (http://glioblastoma.alleninstitute.org/)

In Vivo Study: This study received approval from the Institutional Animal Care and Use Committee (IACUC) of the National Cancer Center research institute. The facility is accredited by the Association for Assessment and Accreditation of Laboratory Animal Care International (AAALAC International) and follows the guidelines outlined by the Institute of Laboratory Animal Resources (ILAR). The approved study number is NCC-17-402. The temperature and humidity in the animal rooms were set and recorded every 10 min, with sensors installed in each room. If the temperature exceeds 25 °C, designated individuals were notified via mobile phone by SMS. The facility operated four cooling units, four air handling units, and a central heating system to maintain the automatic settings. All mice were housed in individually ventilated cages (IVC) with access to food (Altromin, Germany) and autoclaved reverse osmosis (RO) water. The in vivo study was performed as previously described.[25] For the brain orthotopic injection, mice are anesthetized using Zoletil 50 (06516 Carros, France) and cells are suspended in DMEM and DMEM/F-12 supplemented with B27, EGF (10 ng mL^{-1}) and bFGF (5 ng mL^{-1}), and then transplanted into the left striatum of 5-week-old female BALB/c nude mice by stereotactic injection. The injection coordinates were 2.2 mm to the left of the midline and 0.2 mm posterior to the bregma at a depth of 3.5 mm. The brains of each mouse were harvested and fixed in 4% PFA. Bevacizumab (10 mg kg^{-1}; Roche) was administered I.P. every 2 days. Survival was analyzed using GraphPad PRISM software (version 7).

Statistics: All data are presented as mean ± standard error of the mean (SEM) from at least three independent experiments.[23] Survival curves were generated using the Kaplan–Meier method. For patients who were alive at the time of the last follow-up, survival data were censored in the analysis. Statistical analysis was conducted using the Statistical Package for the Social Sciences software (version 16; SPSS, Chicago, IL, USA). For mouse experiments, multiple datasets were compared using analysis of variance (ANOVA) and the log-rank (Mantel–Cox) test. Two-dataset experiments were compared using a two-tailed Student's *t*-test. *p*-values less than 0.05 were considered statistically significant; individual *p*-values are provided in the figure legends.

Supporting Information

Supporting Information is available from the Wiley Online Library or from the author.

Acknowledgements

Y.K. and T.H.K. mainly contributed equally to this work. This work was supported by the research fund of National Cancer Center Graduate School of Cancer Science and Policy (202100320001), the Basic Science Research Program through the National Research Foundation of Korea (NRF) funded by the Ministry of Science and ICT (2021R1A6A3A0108770211), Science Challenge Convergence R&D Project through the National Research Foundation of Korea (NRF) grant funded by the Korea government (MSIT) (2021M3F7A1083230), and the National Research Foundation of Korea (NRF) grant funded by the Korea government (MSIT) (2021R1A2C3013315).

Conflict of Interest

The authors declare no conflict of interest.

Data Availability Statement

The data that support the findings of this study are available from the corresponding author upon reasonable request.

Keywords

bevacizumab resistance, glioblastoma, pseudopalisading cell, translatome

Received: May 3, 2023
Revised: July 7, 2023
Published online: July 28, 2023

[1] K. Chang, B. Zhang, X. Guo, M. Zong, R. Rahman, D. Sanchez, N. Winder, D. A. Reardon, B. Zhao, P. Y. Wen, R. Y. Huang, *Neuro-Oncol.* **2016**, *18*, 1680.
[2] C. Birzu, P. French, M. Caccese, G. Cerretti, A. Idbaih, V. Zagonel, G. Lombardi, *Cancers* **2020**, *13*, 47.
[3] N. Ferrara, K. J. Hillan, H. P. Gerber, W. Novotny, *Nat. Rev. Drug Discovery* **2004**, *3*, 391.
[4] K. R. Hess, E. T. Wong, K. A. Jaeckle, A. P. Kyritsis, V. A. Levin, M. D. Prados, W. K. Yung, *Neuro-Oncol.* **1999**, *1*, 282.
[5] A. D. Norden, J. Drappatz, A. Muzikansky, K. David, M. Gerard, M. B. McNamara, P. Phan, A. Ross, S. Kesari, P. Y. Wen, *J. Neuro-Oncol.* **2009**, *92*, 149.
[6] E. T. Wong, K. R. Hess, M. J. Gleason, K. A. Jaeckle, A. P. Kyritsis, M. D. Prados, V. A. Levin, W. K. Yung, *J. Clin. Oncol.* **1999**, *17*, 2572.
[7] S. D. Rose, M. K. Aghi, *Clin. Neurosurg.* **2010**, *57*, 123.
[8] B. Muz, P. de la Puente, F. Azab, A. K. Azab, *Hypoxia* **2015**, *3*, 83.
[9] M. Brada, *Br. J. Cancer* **2001**, *84*, 148.
[10] P. C. Burger, S. B. Green, *Cancer* **1987**, *59*, 1617.
[11] D. J. Brat, A. A. Castellano-Sanchez, S. B. Hunter, M. Pecot, C. Cohen, E. H. Hammond, S. N. Devi, B. Kaur, E. G. Van Meir, *Cancer Res.* **2004**, *64*, 920.
[12] M. Heiman, R. Kulicke, R. J. Fenster, P. Greengard, N. Heintz, *Nat. Protoc.* **2014**, *9*, 1282.
[13] J. P. Doyle, J. D. Dougherty, M. Heiman, E. F. Schmidt, T. R. Stevens, G. Ma, S. Bupp, P. Shrestha, R. D. Shah, M. L. Doughty, S. Gong, P. Greengard, N. Heintz, *Cell* **2008**, *135*, 749.
[14] M. Heiman, A. Schaefer, S. Gong, J. D. Peterson, M. Day, K. E. Ramsey, M. Suárez-Fariñas, C. Schwarz, D. A. Stephan, D. J. Surmeier, P. Greengard, N. Heintz, *Cell* **2008**, *135*, 738.
[15] M. A. Reynoso, P. Juntawong, M. Lancia, F. A. Blanco, J. Bailey-Serres, M. E. Zanetti, *Methods Mol. Biol.* **2015**, *1284*, 185.
[16] S. Zhang, Y. Chen, Y. Wang, P. Zhang, G. Chen, Y. Zhou, *Front. Genet.* **2020**, *11*, 599548.
[17] A. P. Patel, I. Tirosh, J. J. Trombetta, A. K. Shalek, S. M. Gillespie, H. Wakimoto, D. P. Cahill, B. V. Nahed, W. T. Curry, R. L. Martuza, D. N. Louis, O. Rozenblatt-Rosen, M. L. Suva, A. Regev, B. E. Bernstein, *Science* **2014**, *344*, 1396.
[18] S. Valtorta, D. Salvatore, P. Rainone, S. Belloli, G. Bertoli, R. M. Moresco, *Int. J. Mol. Sci.* **2020**, *21*, 5631.
[19] J. Yin, Y. T. Oh, J. Y. Kim, S. S. Kim, E. Choi, T. H. Kim, J. H. Hong, N. Chang, H. J. Cho, J. K. Sa, J. C. Kim, H. J. Kwon, S. Park, W. Lin, I. Nakano, H. S. Gwak, H. Yoo, S. H. Lee, J. Lee, J. H. Kim, S. Y. Kim, D. H. Nam, M. J. Park, J. B. Park, *Cancer Res.* **2017**, *77*, 4973.
[20] J. Yin, G. Park, J. E. Lee, E. Y. Choi, J. Y. Park, T. H. Kim, N. Park, X. Jin, J. E. Jung, D. Shin, J. H. Hong, H. Kim, H. Yoo, S. H. Lee, Y. J. Kim, J. B. Park, J. H. Kim, *Brain* **2015**, *138*, 2553.
[21] J. Yin, G. Park, J. E. Lee, J. Y. Park, T. H. Kim, Y. J. Kim, S. H. Lee, H. Yoo, J. H. Kim, J. B. Park, *OncoTargets Ther.* **2014**, *5*, 6756.
[22] J. Yin, S. S. Kim, E. Choi, Y. T. Oh, W. Lin, T. H. Kim, J. K. Sa, J. H. Hong, S. H. Park, H. J. Kwon, X. Jin, Y. You, J. H. Kim, H. Kim, J. Son, J. Lee, D. H. Nam, K. S. Choi, B. Shi, H. S. Gwak, H. Yoo, A. Iavarone, J. H. Kim, J. B. Park, *Nat. Commun.* **2020**, *11*, 2978.
[23] J. Yin, G. Park, T. H. Kim, J. H. Hong, Y. J. Kim, X. Jin, S. Kang, J. E. Jung, J. Y. Kim, H. Yun, J. E. Lee, M. Kim, J. Chung, H. Kim, I. Nakano, H. S. Gwak, H. Yoo, B. C. Yoo, J. H. Kim, E. M. Hur, J. Lee, S. H. Lee, M. J. Park, J. B. Park, *PLoS Biol.* **2015**, *13*, e1002152.
[24] W. Lin, R. Niu, S.-M. Park, Y. Zou, S. S. Kim, X. Xia, S. Xing, Q. Yang, X. Sun, Z. Yuan, S. Zhou, D. Zhang, H. J. Kwon, S. Park, C. Il Kim, H. Koo, Y. Liu, H. Wu, M. Zheng, H. Yoo, B. Shi, J. B. Park, J. Yin, *Nat. Commun.* **2023**, *14*, 1578.
[25] a) O. Keunen, M. Johansson, A. Oudin, M. Sanzey, S. A. Rahim, F. Fack, F. Thorsen, T. Taxt, M. Bartos, R. Jirik, H. Miletic, J. Wang, D. Stieber, L. Stuhr, I. Moen, C. B. Rygh, R. Bjerkvig, S. P. Niclou, *Proc. Natl. Acad. Sci. USA* **2011**, *108*, 3749. b) R. Du, K. V. Lu, C. Petritsch, P. Liu, R. Ganss, E. Passegue, H. Song, S. Vandenberg, R. S. Johnson, Z. Werb, G. Bergers, *Cancer Cell* **2008**, *13*, 206.